HHS Public Access

Author manuscript

J Biomed Mater Res A. Author manuscript; available in PMC 2016 February 01.

Published in final edited form as:

J Biomed Mater Res A. 2015 February ; 103(2): 534–544. doi:10.1002/jbm.a.35203.

Scaffold structure and fabrication method affect pro-inflammatory milieu in 3D-cultured chondrocytes

Heenam Kwon[1], **Roshni S. Rainbow**[2], **Lin Sun**[3], **Carrie K. Hui**[1], **Dana M. Cairns**[1], **Rucsanda C. Preda**[4], **David L. Kaplan**[1,3,4], and **Li Zeng**[1,2,5,*]

[1]Program in Cell, Molecular and Developmental Biology, Sackler School of Graduate Biomedical Sciences, Tufts University, 136 Harrison Avenue, Boston, MA 02111, USA

[2]Department of Integrative Physiology and Pathobiology, Tufts University School of Medicine, 136 Harrison Avenue, Boston, MA 02111

[3]Department of Chemical and Biological Engineering, Tufts University, 4 Colby Street, Medford, MA 02155

[4]Department of Biomedical Engineering, Tufts University, 4 Colby Street, Medford, MA 02155

[5]Department of Orthopaedic Surgery, Tufts Medical Center, 800 Washington Street, Boston, MA 02111, USA

Abstract

Cartilage tissue engineering has emerged as an attractive therapeutic option for repairing damaged cartilage tissue in the arthritic joint. High levels of pro-inflammatory cytokines present at arthritic joints can cause cartilage destruction and instability of the engineered cartilage tissue, and thus it is critical to engineer strong and stable cartilage that is resistant to the inflammatory environment. In the present study, we demonstrate that scaffolding materials with different pore sizes and fabrication methods influence the microenvironment of chondrocytes and the response of these cells to pro-inflammatory cytokines, IL-1β and TNFα. Silk scaffolds prepared using the organic solvent hexafluoroisopropanol (HFIP) as compared to an aqueous-based method, as well as those with larger pore sizes, supported the deposition of higher cartilage matrix levels and lower expression of cartilage matrix degradation-related genes, as well as lower expression of endogenous pro-inflammatory cytokines IL-1β in articular chondrocytes. These biochemical properties could be related to the physical properties of the scaffolds such as the water uptake and the tendency to leach or adsorb pro-inflammatory cytokines. Thus, scaffold structure may influence the behavior of chondrocytes by influencing the microenvironment under inflammatory conditions, and should be considered as an important component for bioengineering stable cartilage tissues.

Keywords

cartilage matrix production; scaffold; pro-inflammatory cytokines; cytokine release; water uptake

[*]Corresponding author: Li Zeng (li.zeng@tufts.edu; phone: 617-636-2107, fax: 617-636-3676).

1. Introduction

Osteoarthritis (OA) is a leading debilitating joint disease that has a major public health impact. OA is characterized by the destruction of joint cartilage and is accompanied by inflammation, causing severe pain and immobility[1,2]. Age and obesity are major risk factors for OA. With the increase in obese and aging population, the incidence for OA is becoming ever more prevalent[1,3]. Surgical or pharmacological treatments have been applied to OA patients for symptomatic relief, but they fall short in improving cartilage functions and long-term outcomes[4,5].

Tissue engineering is considered as a potential disease-modifying treatment option for the reconstruction of three-dimensional (3D) tissues that generally involves using cells grown in natural or synthetic scaffolds, which can be eventually transplanted into the host[6–8]. Significant success has been achieved in generating cartilage constructs *in vitro* and transplanting these bioengineered tissues into cartilage defects in animal models *in vivo*[9,10]. However, the stability of engineered cartilage constructs is still not satisfactory. A major reason for this instability is the reduced level of cartilage matrix caused by chondrocyte dedifferentiation or hypertrophy due to mechanical stress and the presence of pro-inflammatory cytokines[6,8,11]. Pro-inflammatory cytokines, most notably interleukin-1beta (IL-1β) and tumor necrosis factor alpha (TNFα), are elevated in the OA cartilage, making it a hostile environment for bioengineered cartilage. These pro-inflammatory cytokines can induce cell death and matrix destruction by downregulating cartilage matrix proteins including aggrecan and type II collagen, and activating proteases such as aggrecanases and matrix metalloproteinases (MMPs)[11–13]. Thus, it is critical to develop strategies to enhance the resistance to IL-1β and TNFα-induced cartilage damage, in order to maintain the stability of the engineered cartilage tissue in the inflammatory environment of OA joint.

Scaffolding is a key component in cartilage tissue engineering as it provides a 3D supportive environment or niche for seeded chondrocytes. Multiple reports demonstrated that chondrocytes produced different amounts of extracellular matrix (ECM) when seeded in scaffolds of different materials, suggesting the importance of selecting optimal scaffolding materials for cartilage formation[14–17]. However, how scaffolds contribute to chondrocyte behavior under inflammatory conditions is largely unknown. Recently, we reported that silk protein scaffolds supported higher levels of ECM under pro-inflammatory cytokine IL-1β and TNFα treatment than collagen and polylactic acid (PLA) scaffolds[18]. However, it was unclear whether the structure of the scaffold would also influence the seeded chondrocytes in terms of their homeostasis in an inflammatory microenvironment.

The present study compares the influence of silk scaffolds of different fabrication methods or pore sizes on chondrocytes under pro-inflammatory cytokines IL-1β and TNFα treatment. Porous silk scaffolds can be generated by an aqueous (AQ) fabrication method or an organic solvent method utilizing hexafluoroisopropanol (HFIP), with each method contributing to differences in the structural architecture and surface morphology of the scaffolds[19–24]. We found that silk scaffolds generated by these two methods, as well as with different pore sizes, supported different levels of pro-inflammatory cytokines and matrix degradation gene expression. Such differences might be related to the different surface characteristics,

cytokine release or adsorption kinetics, and water uptake properties of the scaffolds. We concluded that HFIP silk scaffolds with larger pore sizes maintain a less inflammatory microenvironment, and thus should be considered for engineering stable cartilage tissue under pathological conditions such as OA.

2. Materials and Methods

2.1. Preparation of silk scaffolds

Silk scaffolds were prepared according to our previously described procedures[19,20]. Briefly, cocoons of *Bombyx mori* were boiled for 30 minutes in an aqueous solution of 0.02M Na_2CO_3 and rinsed with distilled water to eliminate sericin. Purified silk fibroin was solubilized in 9.3M LiBr solution and dialyzed against distilled water to generate silk solution. For the study of the comparison between aqueous (AQ) derived and hexafluoroisopropanol (HFIP) derived silk scaffolds, an aqueous solution of 8% (w/v) silk was used to generate scaffolds. AQ silk scaffolds were prepared by adding 4g of NaCl with particle size of 500–600 μm into 2 mL of the silk solution in disk-shaped containers at room temperature. Twenty-four hours later, the containers were immersed in deionized water to extract the salt from the porous scaffolds over 2 days. To generate HFIP silk scaffolds, the obtained aqueous silk solution was lyophilized and the lyophilized silk powder was dissolved in HFIP. Then 3.4 g of NaCl with particle size of 500–600 μm was added into disk-shaped containers and1 mL of the silk-HFIP solution was added over the NaCl. The containers were tightly closed and left in the fume hood for 1–2days for silk-HFIP solution to evenly distribute. The solvent was then evaporated for 2–3 days at room temperature in fume hood. The scaffolds were treated with methanol for 1–2 days and the methanol was evaporated. The scaffolds were then immersed in distilled water for 2 days to extract the salt particles.

For the study comparing different pore sizes in HFIP scaffolds, a solution of 10% (w/v) of silk was used. HFIP silk scaffolds with different pore sizes were prepared as described above utilizing NaCl with particle sizes of 106–212 μm, 300–425 μm, 500–600 μm, and 710–850 μm. The corresponding scaffold pore sizes are referred to as 100–200 μm, 300–400 μm, 500–600 μm, and 700–800 μm, respectively. Pore sizes of all scaffolds were verified by scanning electron microscopy. The porous silk scaffolds were then cut into small disks (5 mm×3 mm (diameter×height)) and autoclaved for cell seeding.

2.2. Isolation of bovine articular chondrocytes

Bovine articular chondrocytes (BACs) were isolated as described previously[25,26]. Articular cartilage from all surfaces of a 2–14day old male calf knee joint (Research 87, Inc. Boylston, MA, USA) was dissected and transferred to a tube containing PBS and 10% penicillin/streptomycin antibiotic mixture. To dissociate articular chondrocytes from the cartilage matrix, minced cartilage pieces were then treated with 1 mg/ml hyaluronidase solution (Sigma, St. Louis, MO, USA) for 15min followed by treatments with 0.25% trypsin solution (Sigma) for 30 min, and 2 mg/ml collagenase solution (Sigma) for approximately 15h at 37°C. The resulting chondrocytes were washed with PBS, resuspended in cell freezing medium (90% Fetal bovine serum (FBS) (Thermo Scientific HyClone, New

Zealand), 10% DMSO (Sigma)), and stored in liquid nitrogen. The purity of the chondrocytes was confirmed by immunocytochemistry for cartilage markers Sox9 and collagen II. Only unpassaged primary cells were used for all experiments.

2.3. Cell seeding and cartilage construct culture

To prepare for cell seeding, all silk scaffolds were presoaked in DMEM (Gibco, Carlsbad, CA, USA) overnight. Chondrocytes were then seeded into these scaffolds at 5×10^4 cells/scaffold. Based on the dimensions of the scaffolds (d=5mm, h=3mm), which would be equivalent to $58.9mm^3$ in total volume, an average seeding density of 0.85×10^3 cells/mm^3scaffold volume can be derived. Note that as the scaffold material occupies a significant amount of space inside the scaffolds, the effective space for cell occupancy is likely to be lower than the calculated scaffold volume. The cell-loaded scaffolds were placed in a humidified tissue culture incubator at 37°C with 5% CO_2 for 2 hr to allow for cell attachment. Scaffolds were then placed in culture medium of DMEM containing 10% FBS, and 1% Antibiotic-antimycotic (Gibco), in the presence or absence of 10 ng/ml of IL-1β or TNFα (Peprotech, Rocky Hill, NJ, USA). These scaffolds were cultured for 8 days or 16 days and medium was changed every 2–3 days. Three independent experiments were carried out.

2.4. Bright field microscopy and scanning electron microscopy (SEM)

Bright field images of scaffolds were taken using Leica MZ 16F microscope and Olympus DP70 digital camera. Top and side views of scaffolds were captured. For SEM analysis, cartilage constructs were fixed in 2.5% gluteraldehyde in 0.1M sodium cacodylate buffer (pH=7.4) at 4°C overnight. The samples were then treated with 1% osmium tetroxide for 1hr, dehydrated in ethanol, and subsequently dried in an Edwards Auto 306 Vacuum Evaporator. The samples were cross sectioned and sputter coated with palladium-gold and cell morphology in cross-sectioned cell-scaffolds was observed using an ISI DS130 scanning electron microscope at the Tufts Imaging Facility and Hitachi S-4800 field emission SEM (FESEM) at Northeastern University.

2.5. RNA isolation and real-time PCR (RT-PCR)

Total RNA from cell-scaffolds was obtained using RNeasy mini kit (Qiagen, Hilden, Germany) according to the manufacturer's protocol. The RNA was reverse transcribed into cDNA using M-MLV reverse transcriptase kit (Invitrogen), random primers (Invitrogen), and dNTPs (New England BioLabs, MA, USA), and stored in −20°C for later analyses. The cDNA was mixed with gene specific primers and SYBR green SuperMix (Quanta Bioscience, Inc., Gaithersburg, MD, USA) and processed for RT-PCR. Gene expression of Col II, Col IX, Aggrecan, IL-1β, IL-6, MMP3, MMP13, ADAMTS4, HIF1α, and HIF2α were quantified using iQ5 Real time PCR Detection system (BioRad, Hercules, CA, USA) and analyzed by iQ5 optical system software. The PCR primers can be found in Supplementary Table 1. All transcript levels were normalized to glyceraldehyde 3-phosphate dehydrogenase (GAPDH) levels.

2.6. Histological staining

After 16 days of culture, cell-loaded scaffolds were fixed in 10% neutral-buffered formalin and embedded in paraffin for histological evaluation. The embedded samples were sectioned at 5μm thickness and then processed and stained with hematoxylin and eosin (H&E) and toluidine blue using standard protocols.

2.7. Cytokine release kinetics analysis

Pro-inflammatory cytokines IL-1β or TNFα (Peprotech) were loaded onto prewetted scaffolds at the following amount: 1 ng, or 10 ng, in 10 μl of medium. The loaded scaffolds were incubated for 6 hr at room temperature, immersed into 1ml of culture medium, and placed in a humidified tissue culture incubator at 37°C with 5% CO_2. At each time point (10 min, 1hr, 1d, and 3d), scaffolds were transferred into fresh media, and the remaining media were collected and stored in −80°C for later analysis. The initial loading amount and concentrations of pro-inflammatory cytokines at all time points present in the collected media samples were quantified using ELISA (Quantikine; R&D Systems, Minneapolis, MN, USA). Percent release was calculated as the ratio of the amount of cytokines in the medium to the initial amount of cytokines loaded onto the scaffolds. Percent cumulative release was calculated as the ratio of cumulative amount of cytokines in the medium at each time point (i.e. sum cytokine amount at each time point and all prior time points) to the initial amount of cytokines loaded onto the scaffolds.

2.8. Analysis of water uptake abilities of the scaffolds

The water uptake of AQ and HFIP silk scaffolds was determined using a previously established protocol[20]. Scaffolds were immersed in distilled water for 24 hours at room temperature. The wet weight of the scaffolds (W_{wet}) was measured after removing excess water from the scaffolds. The scaffolds were then dried in an oven at 65°C overnight and the weight of dried scaffolds (W_{dry}) was then measured. The water uptake (%) values were obtained using the following formula:

$$\text{Water uptake (\%)} = \{(W_{wet} - W_{dry}) / W_{wet}\} \times 100.$$

2.9. Statistical analysis

Data was presented as mean ± SD with a minimum of three samples. To determine the statistical differences for gene expression and water uptake between AQ and HFIP scaffolds and different pore-sized HFIP scaffolds for the same treatment, data was analyzed by t-test and one-way ANOVA with post-hoc Tukey test (GraphPad Prism; http://www.graphad.com), respectively. For the cytokine release analysis, two-way ANOVA with a Bonferroni post test was used to determine the statistical difference among the materials over time. $*p < 0.05$ was considered statistically significant.

3. Results

3.1. HFIP silk scaffolds supported higher levels of cartilage matrix production and a lower level of matrix degradation in 3D cultured chondrocytes

To determine whether silk scaffolds generated by different fabrication methods affected their abilities to support chondrocyte gene expression under inflammatory conditions, we analyzed primary bovine articular chondrocytes grown in porous silk scaffolds generated by the AQ or HFIP methods. SEM analysis showed that while these scaffolds have the same pore size (500–600 μm), the pores of cell-free AQ silk scaffolds had rougher surfaces than those of HFIP silk scaffolds (Fig.1A and 1B). Interestingly, chondrocytes in AQ silk scaffolds were flatter than those in the HFIP scaffolds (Fig. 1C–1E). We performed toluidine blue staining to evaluate cartilage matrix deposition. Toluidine blue is a basic dye that exhibits a color shift toward the violet-purple range (i. e. metachromasia) when the level of glycosyamonioglycan (GAG) is high[18]. Significantly, a much stronger and metachromatic toluidine blue staining was observed in chondrocytes grown in the HFIP silk scaffolds than in the AQ silk scaffolds under the control conditions, suggesting a higher level of matrix deposition in the HFIP scaffolds (Fig. 1F). While IL-1β and TNFα treatments reduced the intensity of toluidine blue staining in all scaffolds, the staining was still stronger around chondrocytes grown in the HFIP scaffolds than in the AQ-silk scaffolds (Fig. 1F).

To provide a more quantitative measure for such differences and to determine whether the difference in matrix production was caused by a difference in gene expression, we performed real time PCR (qRT-PCR) to assess cartilage matrix and degradation-related genes. We examined the expression of cartilage matrix genes collagen II (Col II), collagen IX (Col IX) and aggrecan. We also examined the expression of pro-inflammatory cytokines IL-1β and IL-6, both which are known to promote the expression of cartilage degradation genes such as MMP3, MMP13 and ADAMTSs[27–29]. Initially at day 8, IL-1β-treated chondrocytes grown in HFIP silk scaffolds showed a slightly higher levels of Col II, aggrecan, and also higher levels of endogenous IL-1β, MMP13 and ADAMTS5 than those in AQ-silk scaffold. However, no differences were observed in control and TNFα-treated samples (Fig. 2A). At day 16, chondrocytes grown in HFIP silk exhibited higher levels of cartilage matrix genes and lower levels of IL-6 and MMP3 than those in AQ-silk scaffolds under the control condition (Fig. 2B). Furthermore, the level of MMP3 was significantly lower in the HFIP-silk scaffolds in IL-1β or TNFα-treated samples (Fig. 2B).

To investigate whether these differences in gene expression could be due to the differences in important transcription factors of chondrogenesis, we examined the expression of Sox9, Runx2 as well as HIF1α and HIF2α. Sox9 is known to promote cartilage matrix genes collagen II, collagen IV and aggrecan, while Runx2 promotes chondrocyte hypertrophy-related genes collagen X and MMPs[30–33]. We did not observe any differences in Sox9 and Runx2 expression among the samples, suggesting that altered cartilage gene expression was mediated by other factors (data not shown). HIF1α and HIF2α are hypoxia-induced transcription factors that play important roles in regulating cartilage gene expression. HIF1α promotes the expression of cartilage matrix genes, and thereby, is beneficial to cartilage, while HIF2α promotes the expression of matrix degradation genes and induces OA, thus it is

detrimental to cartilage[34–36]. While there was no difference in HIF1α expression, we did observe that chondrocytes cultured in HFIP scaffolds at day 16 showed significantly lower levels of HIF2α in control and TNFα-treated samples (Fig. 2B)[35]. This finding was consistent with the observation that there were lower levels of pro-inflammatory cytokines and MMPs in HFIP scaffolds (Fig. 2). Since we did not observe any differences in the expression of HIF1α at any time point, it suggests that there was no difference in oxygen levels in AQ and HFIP scaffolds. Although we observed lower levels of IL-1β and IL-6 in HFIP scaffolds under TNFα treatment (Fig. 2B), we did not detect significant levels of TNFα expression itself in any conditions, suggesting that TNFα did not induce its own expression in our system (data not shown). Overall, the gene expression analysis was consistent with the observed higher level of matrix deposition in HFIP silk scaffolds, suggesting that the HFIP scaffolds were more suitable for maintaining cartilage features.

3.2. Scaffold pore-size influences the pro-inflammatory micronenvironment in 3D cultured chondrocytes

We next investigated whether scaffold pore size influenced cartilage matrix production and gene expression under control and inflammatory conditions. Based on the data shown in Section 3.1, we chose to use HFIP-silk scaffolds for this analysis. In addition to the 500–600 μm pore size, which we used earlier in comparison with AQ-silk scaffolds, we also included three other pore sizes: 100–200, 300–400, and 700–800 μm (Fig.3A and 3B). SEM confirmed the pore sizes of these scaffolds, but did not reveal any significant differences among cells grown in the scaffolds (Fig.3C and 3D). H&E and toluidine blue staining analyses from day 16 cultures showed that chondrocytes in the different scaffolds had similar cell shapes and did not exhibit obvious differences in matrix levels (Fig. 3E–3F).

Gene expression analysis from 8- and 16-day cultures indicated that while there was no major difference in the expression of cartilage matrix genes (Col II, Col IX, and aggrecan), there were significant differences in the expression of cartilage degradation-related genes in cells grown in these different scaffolds (Fig.4A and 4B). In general, larger pore-sized scaffolds supported less MMP3, MMP13 as well as ADAMTS4 expression. Correspondingly, there were lower levels of endogenous pro-inflammatory cytokine IL-1β and IL-6 expression, as well as cartilage degradation promoter factor HIF2α, in large pore-sized scaffolds. This suggested that larger pore-sized silk scaffolds supported lower levels of matrix degradation than smaller pore-sized scaffolds. Interestingly, we did observe a higher level of HIF1α in the smallest pore sized scaffolds than the other larger pore-sized scaffolds at day 16 in the control condition, which may indicate that as chondrocytes grew, the microenvironment in smaller pore sized scaffolds became more hypoxic (Fig.4A and 4B). We did not observe any differences in HIF1α expression in conditions of pro-inflammatory cytokine treatment. Perhaps the cell density under pro-inflammatory cytokine treatment was not high enough to reach a hypoxic state even in the smaller pore-sized scaffolds.

3.3. Different silk scaffolds have different profiles of pro-inflammatory cytokine release and water uptake ability

To investigate why scaffolds derived from various fabrication methods with a range of structural properties would result in differential endogenous pro-inflammatory cytokine

levels or cartilage matrix gene expression under inflammatory conditions, we examined the ability of the scaffolds to adsorb and release pro-inflammatory cytokines. We reasoned that the difference in scaffold structures might cause a difference in the diffusion of the cytokines between the scaffolds and the medium, which would lead to a difference in the inflammatory microenvironment surrounding the seeded chondrocytes[18]. Thus, we applied equal amounts of the cytokines to AQ scaffolds, HFIP scaffolds, and HFIP scaffolds with different pore sizes and then evaluated the amount of cytokines that leached out the scaffolds into the medium. As we were uncertain of the capacity of the scaffolds to adsorb IL-1β or TNFα, we applied two different amounts (1ng and 10ng) to the scaffolds and assayed the medium at different time points using ELISA (Fig. 5). We found that IL-1β and TNFα were released from HFIP silk scaffolds at a faster rate than the AQ silk scaffolds (Fig. 5A and 5B). At 10 mins, 70% of IL-1β and 60% of TNFα were released by HFIP silk scaffolds, while only 40% of IL-1β or TNFα were released by AQ silk scaffolds, suggesting that HFIP scaffolds retained less IL-1β and TNFα than the AQ scaffolds (Fig.5A and 5B). With respect to scaffolds of different pore sizes, larger pore-sized scaffolds released more IL-1β and TNFα than smaller pore-sized scaffolds, which may be related to the lower physical barrier present in larger pore sized scaffolds (Fig.5C and 5D). This result is consistent with the fact that HFIP silk scaffolds with larger pore sizes supported a lower level of endogenous IL-1β and IL-6 even in the absence of exogenously administered pro-inflammatory cytokines, which correlates with lower levels of matrix degradation-associated genes in larger pore-sized scaffolds. Another scaffold property that may affect the microenvironment of the chondrocytes is the ability to uptake water, which is correlated with the hydrophilicity of the material. The degree of hydration in the microenvironment could determine the local concentration of nutrients or pro-inflammatory cytokines, which in turn could affect chondrocyte gene expression. We found that HFIP silk scaffolds had a higher ability to retain water than AQ silk scaffolds, suggesting that HFIP silk scaffolds may establish a more hydrated microenvironment for the chondrocytes (Fig. 5E). Expectedly, HFIP silk scaffolds of different pore size did not have differential water uptake abilities, as they were derived from same scaffold material using the same preparation method (Fig. 5F).

4. Discussion

The relationship between inflammation and regeneration is intriguing. For some tissues and processes, such as during zebrafish neuron regeneration or fracture healing of the bone, the response to inflammatory stimuli is essential[37,38]. However, prolonged inflammation could be damaging to the tissues[39,40]. Unlike many vascularized tissues, the avascular cartilage has poor regeneration ability. Joint injury (such as ACL or meniscus tear) is accompanied by high levels of inflammation, which although this subsides over time, may have a profound effect on chondrocyte homeostasis[41–43]. Many cartilage injuries lead to osteoarthritis (OA) years later[44,45]. Significantly higher levels of pro-inflammatory cytokines IL-1β and TNFα were found in early OA joints[46]. However, higher levels of other pro-inflammatory mediators such as IL-6 and leptin were reported to be predominant in end stage OA synovial fluid[47]. Such localized inflammation will compromise the stability of the cartilage[48,49]. Therefore, it is important to engineer stable cartilage under inflammatory conditions.

Scaffolding constitutes an integral component of the microenvironment architecture for chondrocytes in 3D bioengineered cartilage constructs. However, the function of scaffolding on cartilage gene expression in the arthritic inflammatory environment still remains largely elusive. We chose silk scaffolds for this study because our previous work had revealed that silk supported higher levels of cartilage matrix deposition than collagen and PLA scaffolds under pro-inflammatory cytokine treatment[18]. Here we found that silk scaffolds prepared by HFIP and those with larger pore sizes supported higher levels of cartilage matrix than those prepared by the AQ method or with smaller pore sizes. Interestingly, we did observe that HFIP scaffolds also supported higher levels of MMP13 and ADAMTS4 in the presence of IL-1β at 8 days. It is possible that chondrocytes grown in the HFIP silk scaffold might be more metabolically active and more readily in participating in a repair response under IL-1β treatment than those in AQ silk scaffolds. As at the later time point of 16 days, we observed lower MMP13 and ADAMTS4 expression in HFIP scaffolds, it suggests that the initial increase in these catabolic genes did not last, and eventually chondrocytes in the HFIP scaffolds had a higher matrix production/matrix degradation ratio in terms of gene expression.

Our results are consistent with previous studies in demonstrating that different cell types exhibit varied differentiation potential in AQ and HFIP silk scaffolds. For example, for osteogenesis, it was shown that AQ silk scaffolds supported more optimal osteogenic differentiation from human mesenchymal stem cells (hMSCs), while for dental pulp progenitor cells, HFIP silk scaffolds are more favorable[24,51]. For elastic cartilage, a higher overall matrix deposition was found in sucrose/HFIP scaffolds than in AQ silk scaffolds[52]. We have analyzed the difference in gene expression in chondrocytes from AQ and HFIP scaffolds under normal conditions, and further extended our investigation to inflammatory conditions. We found that HFIP scaffolds supported less endogenous pro-inflammatory cytokine expression and the cartilage-degradation-related genes in chondrocytes. Therefore, the preference for selecting fabrication methods has to be determined based on cell type and biological processes.

While the effect of pore size on chondrocyte gene expression in the silk scaffolds has not been carried out, there are reports that indicate that pore sizes of other types of scaffolds can affect cartilage gene expression[53–58]. For example, chondrocytes isolated from newborn rats exhibited a higher level of collagen II expression in larger pore-sized gelatin scaffolds than in smaller pore-sized scaffolds; but interestingly, they also expressed higher levels of dedifferentiation marker collagen I and hypertrophic marker collagen X[53]. We did not observed any difference in the expression of hypertrophic markers Runx2 and collagen X under normal or inflammatory conditions, suggesting that scaffold pore size does not affect chondrocyte hypertrophy in our culture system. A limitation of our matrix analysis is that we did not assess the total GAG content of the entire scaffolds. Future studies to determine GAG contents in higher seeding density and long-term cultures will be highly desirable.

Scaffolds seem to alter gene expression through their unique chemical and physical characteristics[61–63]. Our data shows that HFIP silk scaffolds have smoother surfaces than AQ silk scaffolds, which is consistent with prior studies[20,52]. AQ silk scaffolds are more rigid, while HFIP silk scaffolds are more elastic and deformable[20,24,52]. Such mechanical

property could be related to the water uptake ability or swelling ratio of the scaffolds, which is indicative of hydrophilicity[64–66]. Previous studies have shown that hydrophilic scaffolds supported better cartilage formation through enhanced collagen type II expression and cell redifferentiation in chondrocytes[67–69]. It is possible that higher hydrophilicity allows for optimal function of the ECM, and thus higher levels of matrix production. However, hydrophilicity or water uptake ability is only one aspect of the scaffold. We did not observe any differences in water uptake in different pore sized silk scaffolds, even though we observed a difference in cartilage gene expression. Therefore, other biophysical aspects of the scaffolds certainly contribute to the differential gene expression.

We also have investigated the property of scaffolds in retaining and releasing pro-inflammatory cytokines. We reasoned that when equal amount of pro-inflammatory cytokines were applied to the scaffold, the faster that the cytokines leached into the medium, the less cytokines would be left within the scaffold microenvironment for the chondrocytes to encounter. While the protein release profile from the scaffolds has been studied for other proteins such as BMP-2, VEGF, and IGF-I, it has rarely been attempted for pro-inflammatory cytokines[70–74]. In our prior analysis on different scaffolding materials, faster leaching of the pro-inflammatory cytokine was found to be correlated with higher level of cartilage matrix production[18]. Here, we found it also to be case for silk scaffolds of different fabrication methods and pore sizes. HFIP scaffolds (vs. AQ scaffolds) and larger pore sized HFIP scaffolds (vs. smaller pore sized scaffolds) released IL-1β and TNFα at a faster rate, and supported higher levels of cartilage matrix. It is not clear why HFIP-silk scaffolds leach the cytokines faster than AQ-silk scaffolds. It could be related to the smoother surface characteristics of the HFIP scaffolds or the distinct structure and surface chemistry of the scaffolds. With respect to pore size, it can be surmised that larger pore size would allow pro-inflammatory cytokines to pass more freely, resulting in faster leaching of the cytokines into the medium.

Interestingly, even in the absence of exogenous IL-1β and TNFα, there was a difference in chondrocyte gene expression. This may be related to the level of endogenous IL-1β expression, which was lowest in HFIP scaffolds (vs. AQ) and those with larger pore sizes (vs. smaller pore sizes). IL-1β is able to induce its own expression, as well as other pro-inflammatory cytokines (such as IL-6) and cartilage degradation related genes MMPs and HIF2[27,35,75]. Furthermore, IL-6 in turn mediates HIF2α-induced cartilage destruction[76]. Thus faster release of IL-1β from the scaffold to the medium, be it endogenous or exogenous, may be beneficial to cartilage matrix maintenance. Thus, this property may be an important component of the scaffold as the chondrocyte niche. In the cytokine release analysis, we had observed the same trend of cytokine release kinetics when different amount of cytokines were applied. However, in the disease conditions, the levels of these cytokines may differ among individuals. A limitation in our study is that our cytokine release study had analyzed cytokines leached from the scaffolds to the medium, which, although mimicking the course of diffusion of cytokines such as IL-1β endogenously produced by the chondrocytes, did not directly assess the diffusion of exogenous cytokines from the medium to the scaffolds. Studies using radiolabeled cytokines would be desirable to specifically address this question. Certainly, other properties of scaffolding material, including rigidity, degradation rate may also contribute to the chondrocyte niche in regulating the response of

chondrocytes to inflammatory stimuli. The mechanical property of the engineered cartilage is critical to its function, and IL-1β is known to impair such function[77]. In future studies, it will also be important to evaluate the biomechanical properties of cartilage constructs in long-term cultures to correlate matrix gene expression with the functionality of the bioengineered cartilage.

5. Conclusions

The present study demonstrates that scaffold fabrication method and structure contribute to the inflammatory environment and regulate the cellular response of chondrocytes toward pro-inflammatory cytokines. Silk scaffolds prepared by HFIP organic solvent method and those with larger pore sizes supported higher levels of cartilage matrix than those prepared by the AQ method or with smaller pore sizes. Interestingly, HFIP-silk scaffolds with larger pore sizes also have a higher tendency to leach pro-inflammatory cytokines into the medium, which may influence cartilage gene expression. As scaffolding has intimate contact with the chondrocytes, it is an important component of the chondrocyte cell niche. By manipulating chemical, physical, and structural properties of scaffolds, we may be able to select the optimal scaffold to provide the appropriate microenvironment for engineering stable cartilage tissue under pathological conditions.

Supplementary Material

Refer to Web version on PubMed Central for supplementary material.

ACKNOWLEDGMENTS

We are grateful for Catherine Linsenmayer at Tufts imaging facility for help with the scanning electron microscopy. This work has been supported by grants to LZ and DLK from the NSF (CBET-0966920) and NIH (1R01AR059106-01A1), as well as a postdoctoral fellowship NIH/NIGMS (K12GM074869) to RR.

References

1. Bijlsma JW, Berenbaum F, Lafeber FP. Osteoarthritis: an update with relevance for clinical practice. Lancet. 2011; 377(9783):2115–2126. [PubMed: 21684382]
2. Pelletier JP, Martel-Pelletier J, Abramson SB. Osteoarthritis, an inflammatory disease: potential implication for the selection of new therapeutic targets. Arthritis and rheumatism. 2001; 44(6): 1237–1247. [PubMed: 11407681]
3. Clouet J, Vinatier C, Merceron C, Pot-vaucel M, Maugars Y, Weiss P, Grimandi G, Guicheux J. From osteoarthritis treatments to future regenerative therapies for cartilage. Drug discovery today. 2009; 14(19–20):913–925. [PubMed: 19651235]
4. Shah MR, Kaplan KM, Meislin RJ, Bosco JA 3rd. Articular cartilage restoration of the knee. Bull NYU Hosp Jt Dis. 2007; 65(1):51–60. [PubMed: 17539762]
5. Smith GD, Knutsen G, Richardson JB. A clinical review of cartilage repair techniques. The Journal of bone and joint surgery. British volume. 2005; 87(4):445–449. [PubMed: 15795189]
6. Hunziker EB. Articular cartilage repair: basic science and clinical progress. A review of the current status and prospects. Osteoarthritis Cartilage. 2002; 10(6):432–463. [PubMed: 12056848]
7. Chung C, Burdick JA. Engineering cartilage tissue. Adv Drug Deliv Rev. 2008; 60(2):243–262. [PubMed: 17976858]
8. Vinatier C, Mrugala D, Jorgensen C, Guicheux J, Noel D. Cartilage engineering: a crucial combination of cells, biomaterials and biofactors. Trends Biotechnol. 2009; 27(5):307–314. [PubMed: 19329205]

9. Tang QO, Carasco CF, Gamie Z, Korres N, Mantalaris A, Tsiridis E. Preclinical and clinical data for the use of mesenchymal stem cells in articular cartilage tissue engineering. Expert Opin Biol Ther. 12(10):1361–1382. [PubMed: 22784026]
10. Johnstone B, Alini M, Cucchiarini M, Dodge GR, Eglin D, Guilak F, Madry H, Mata A, Mauck RL, Semino CE, et al. Tissue engineering for articular cartilage repair--the state of the art. Eur Cell Mater. 25:248–267. [PubMed: 23636950]
11. Steinert AF, Ghivizzani SC, Rethwilm A, Tuan RS, Evans CH, Noth U. Major biological obstacles for persistent cell-based regeneration of articular cartilage. Arthritis Res Ther. 2007; 9(3):213. [PubMed: 17561986]
12. Amin AR, Dave M, Attur M, Abramson SB. COX-2, NO, and cartilage damage and repair. Current rheumatology reports. 2000; 2(6):447–453. [PubMed: 11123096]
13. Lotz M. Cytokines in cartilage injury and repair. Clin Orthop Relat Res. 2001; (391 Suppl):S108–S115. [PubMed: 11603695]
14. Schlegel W, Nurnberger S, Hombauer M, Albrecht C, Vecsei V, Marlovits S. Scaffold-dependent differentiation of human articular chondrocytes. Int J Mol Med. 2008; 22(5):691–699. [PubMed: 18949392]
15. Jeong CG, Hollister SJ. A comparison of the influence of material on in vitro cartilage tissue engineering with PCL, PGS, and POC 3D scaffold architecture seeded with chondrocytes. Biomaterials. 2010; 31(15):4304–4312. [PubMed: 20219243]
16. Schagemann JC, Kurz H, Casper ME, Stone JS, Dadsetan M, Yu-Long S, Mrosek EH, Fitzsimmons JS, O'Driscoll SW, Reinholz GG. The effect of scaffold composition on the early structural characteristics of chondrocytes and expression of adhesion molecules. Biomaterials. 2010
17. Appelman TP, Mizrahi J, Elisseeff JH, Seliktar D. The influence of biological motifs and dynamic mechanical stimulation in hydrogel scaffold systems on the phenotype of chondrocytes. Biomaterials. 2011; 32(6):1508–1516. [PubMed: 21093907]
18. Kwon H, Sun L, Cairns DM, Rainbow RS, Preda RC, Kaplan DL, Zeng L. The influence of scaffold material on chondrocytes under inflammatory conditions. Acta biomaterialia. 2013
19. Nazarov R, Jin HJ, Kaplan DL. Porous 3-D scaffolds from regenerated silk fibroin. Biomacromolecules. 2004; 5(3):718–726. [PubMed: 15132652]
20. Kim UJ, Park J, Kim HJ, Wada M, Kaplan DL. Three-dimensional aqueous-derived biomaterial scaffolds from silk fibroin. Biomaterials. 2005; 26(15):2775–2785. [PubMed: 15585282]
21. Meinel L, Hofmann S, Karageorgiou V, Zichner L, Langer R, Kaplan D, Vunjak-Novakovic G. Engineering cartilage-like tissue using human mesenchymal stem cells and silk protein scaffolds. Biotechnol Bioeng. 2004; 88(3):379–391. [PubMed: 15486944]
22. Meinel L, Karageorgiou V, Hofmann S, Fajardo R, Snyder B, Li C, Zichner L, Langer R, Vunjak-Novakovic G, Kaplan DL. Engineering bone-like tissue in vitro using human bone marrow stem cells and silk scaffolds. J Biomed Mater Res A. 2004; 71(1):25–34. [PubMed: 15316936]
23. Vunjak-Novakovic G, Altman G, Horan R, Kaplan DL. Tissue engineering of ligaments. Annu Rev Biomed Eng. 2004; 6:131–156. [PubMed: 15255765]
24. Zhang W, Ahluwalia IP, Literman R, Kaplan DL, Yelick PC. Human dental pulp progenitor cell behavior on aqueous and hexafluoroisopropanol based silk scaffolds. J Biomed Mater Res A. 97(4):414–422. [PubMed: 21484985]
25. Mauck RL, Seyhan SL, Ateshian GA, Hung CT. Influence of seeding density and dynamic deformational loading on the developing structure/function relationships of chondrocyte-seeded agarose hydrogels. Ann Biomed Eng. 2002; 30(8):1046–1056. [PubMed: 12449765]
26. Cairns D, Lee P, Uchimura T, Seufert C, Kwon H, Zeng L. The role of muscle cells in regulating cartilage matrix production. J Orthop Res. 2010; 28(4):529–536. [PubMed: 19813241]
27. Fernandes JC, Martel-Pelletier J, Pelletier JP. The role of cytokines in osteoarthritis pathophysiology. Biorheology. 2002; 39(1–2):237–246. [PubMed: 12082286]
28. Flannery CR, Little CB, Hughes CE, Curtis CL, Caterson B, Jones SA. IL-6 and its soluble receptor augment aggrecanase-mediated proteoglycan catabolism in articular cartilage. Matrix Biol. 2000; 19(6):549–553. [PubMed: 11068209]

29. Shi J, Schmitt-Talbot E, DiMattia DA, Dullea RG. The differential effects of IL-1 and TNF-alpha on proinflammatory cytokine and matrix metalloproteinase expression in human chondrosarcoma cells. Inflamm Res. 2004; 53(8):377–389. [PubMed: 15316669]
30. Bell DM, Leung KK, Wheatley SC, Ng LJ, Zhou S, Ling KW, Sham MH, Koopman P, Tam PP, Cheah KS. SOX9 directly regulates the type-II collagen gene. Nat Genet. 1997; 16(2):174–178. [PubMed: 9171829]
31. Bi W, Deng JM, Zhang Z, Behringer RR, de Crombrugghe B. Sox9 is required for cartilage formation. Nat Genet. 1999; 22(1):85–89. [PubMed: 10319868]
32. Wang X, Manner PA, Horner A, Shum L, Tuan RS, Nuckolls GH. Regulation of MMP-13 expression by RUNX2 and FGF2 in osteoarthritic cartilage. Osteoarthritis Cartilage. 2004; 12(12): 963–973. [PubMed: 15564063]
33. Kamekura S, Kawasaki Y, Hoshi K, Shimoaka T, Chikuda H, Maruyama Z, Komori T, Sato S, Takeda S, Karsenty G, et al. Contribution of runt-related transcription factor 2 to the pathogenesis of osteoarthritis in mice after induction of knee joint instability. Arthritis Rheum. 2006; 54(8): 2462–2470. [PubMed: 16868966]
34. Yudoh K, Nakamura H, Masuko-Hongo K, Kato T, Nishioka K. Catabolic stress induces expression of hypoxia-inducible factor (HIF)-1 alpha in articular chondrocytes: involvement of HIF-1 alpha in the pathogenesis of osteoarthritis. Arthritis Res Ther. 2005; 7(4):R904–R914. [PubMed: 15987493]
35. Yang S, Kim J, Ryu JH, Oh H, Chun CH, Kim BJ, Min BH, Chun JS. Hypoxia-inducible factor-2alpha is a catabolic regulator of osteoarthritic cartilage destruction. Nat Med. 16(6):687–693. [PubMed: 20495569]
36. Lafont JE, Talma S, Murphy CL. Hypoxia-inducible factor 2alpha is essential for hypoxic induction of the human articular chondrocyte phenotype. Arthritis Rheum. 2007; 56(10):3297–3306. [PubMed: 17907154]
37. Kyritsis N, Kizil C, Zocher S, Kroehne V, Kaslin J, Freudenreich D, Iltzsche A, Brand M. Acute inflammation initiates the regenerative response in the adult zebrafish brain. Science. 338(6112): 1353–1356. [PubMed: 23138980]
38. Mountziaris PM, Mikos AG. Modulation of the inflammatory response for enhanced bone tissue regeneration. Tissue Eng Part B Rev. 2008; 14(2):179–186. [PubMed: 18544015]
39. Abou-Khalil R, Yang F, Mortreux M, Lieu S, Yu YY, Wurmser M, Pereira C, Relaix F, Miclau T, Marcucio RS, et al. Delayed bone regeneration is linked to chronic inflammation in murine muscular dystrophy. J Bone Miner Res.
40. Hardy R, Cooper MS. Bone loss in inflammatory disorders. J Endocrinol. 2009; 201(3):309–320. [PubMed: 19443863]
41. Irie K, Uchiyama E, Iwaso H. Intraarticular inflammatory cytokines in acute anterior cruciate ligament injured knee. The Knee. 2003; 10(1):93–96. [PubMed: 12649034]
42. Marks PH, Donaldson ML. Inflammatory cytokine profiles associated with chondral damage in the anterior cruciate ligament-deficient knee. Arthroscopy : the journal of arthroscopic & related surgery : official publication of the Arthroscopy Association of North America and the International Arthroscopy Association. 2005; 21(11):1342–1347.
43. Ochi M, Uchio Y, Okuda K, Shu N, Yamaguchi H, Sakai Y. Expression of cytokines after meniscal rasping to promote meniscal healing. Arthroscopy : the journal of arthroscopic & related surgery : official publication of the Arthroscopy Association of North America and the International Arthroscopy Association. 2001; 17(7):724–731.
44. Murray MM, Fleming BC. Biology of anterior cruciate ligament injury and repair: Kappa delta ann doner vaughn award paper 2013. Journal of orthopaedic research : official publication of the Orthopaedic Research Society. 2013; 31(10):1501–1506. [PubMed: 23818453]
45. Li RT, Lorenz S, Xu Y, Harner CD, Fu FH, Irrgang JJ. Predictors of radiographic knee osteoarthritis after anterior cruciate ligament reconstruction. The American journal of sports medicine. 2011; 39(12):2595–2603. [PubMed: 22021585]
46. Smith MD, Triantafillou S, Parker A, Youssef PP, Coleman M. Synovial membrane inflammation and cytokine production in patients with early osteoarthritis. The Journal of rheumatology. 1997; 24(2):365–371. [PubMed: 9034998]

47. Beekhuizen M, Gierman LM, van Spil WE, Van Osch GJ, Huizinga TW, Saris DB, Creemers LB, Zuurmond AM. An explorative study comparing levels of soluble mediators in control and osteoarthritic synovial fluid. Osteoarthritis and cartilage / OARS, Osteoarthritis Research Society. 2013; 21(7):918–922.
48. van der Kraan PM. Osteoarthritis year 2012 in review: biology. Osteoarthritis and cartilage / OARS, Osteoarthritis Research Society. 2012; 20(12):1447–1450.
49. Loeser RF. Osteoarthritis year in review 2013: biology. Osteoarthritis and cartilage / OARS, Osteoarthritis Research Society. 2013; 21(10):1436–1442.
50. Aigner T, Soeder S, Haag J. IL-1beta and BMPs--interactive players of cartilage matrix degradation and regeneration. Eur Cell Mater. 2006; 12:49–56. discussion 56. [PubMed: 17068722]
51. Kim HJ, Kim UJ, Vunjak-Novakovic G, Min BH, Kaplan DL. Influence of macroporous protein scaffolds on bone tissue engineering from bone marrow stem cells. Biomaterials. 2005; 26(21): 4442–4452. [PubMed: 15701373]
52. Makaya K, Terada S, Ohgo K, Asakura T. Comparative study of silk fibroin porous scaffolds derived from salt/water and sucrose/hexafluoroisopropanol in cartilage formation. J Biosci Bioeng. 2009; 108(1):68–75. [PubMed: 19577196]
53. Lien SM, Ko LY, Huang TJ. Effect of pore size on ECM secretion and cell growth in gelatin scaffold for articular cartilage tissue engineering. Acta Biomater. 2009; 5(2):670–679. [PubMed: 18951858]
54. Oh SH, Park IK, Kim JM, Lee JH. In vitro and in vivo characteristics of PCL scaffolds with pore size gradient fabricated by a centrifugation method. Biomaterials. 2007; 28(9):1664–1671. [PubMed: 17196648]
55. Bhardwaj T, Pilliar RM, Grynpas MD, Kandel RA. Effect of material geometry on cartilagenous tissue formation in vitro. J Biomed Mater Res. 2001; 57(2):190–199. [PubMed: 11484181]
56. Schwartz Z, Martin JY, Dean DD, Simpson J, Cochran DL, Boyan BD. Effect of titanium surface roughness on chondrocyte proliferation, matrix production, and differentiation depends on the state of cell maturation. J Biomed Mater Res. 1996; 30(2):145–155. [PubMed: 9019478]
57. El-Ayoubi R, DeGrandpre C, DiRaddo R, Yousefi AM, Lavigne P. Design and dynamic culture of 3D-scaffolds for cartilage tissue engineering. J Biomater Appl. 25(5):429–444. [PubMed: 20042429]
58. Stenhamre H, Nannmark U, Lindahl A, Gatenholm P, Brittberg M. Influence of pore size on the redifferentiation potential of human articular chondrocytes in poly(urethane urea) scaffolds. J Tissue Eng Regen Med. 5(7):578–588. [PubMed: 21695799]
59. O'Brien FJ, Harley BA, Yannas IV, Gibson LJ. The effect of pore size on cell adhesion in collagen-GAG scaffolds. Biomaterials. 2005; 26(4):433–441. [PubMed: 15275817]
60. Oh S, Brammer KS, Li YS, Teng D, Engler AJ, Chien S, Jin S. Stem cell fate dictated solely by altered nanotube dimension. Proc Natl Acad Sci U S A. 2009; 106(7):2130–2135. [PubMed: 19179282]
61. Boyan BD, Hummert TW, Dean DD, Schwartz Z. Role of material surfaces in regulating bone and cartilage cell response. Biomaterials. 1996; 17(2):137–146. [PubMed: 8624390]
62. Miot S, Woodfield T, Daniels AU, Suetterlin R, Peterschmitt I, Heberer M, van Blitterswijk CA, Riesle J, Martin I. Effects of scaffold composition and architecture on human nasal chondrocyte redifferentiation and cartilaginous matrix deposition. Biomaterials. 2005; 26(15):2479–2489. [PubMed: 15585250]
63. Arima Y, Iwata H. Effect of wettability and surface functional groups on protein adsorption and cell adhesion using well-defined mixed self-assembled monolayers. Biomaterials. 2007; 28(20): 3074–3082. [PubMed: 17428532]
64. Lou X, Chirila TV. Swelling behavior and mechanical properties of chemically cross-linked gelatin gels for biomedical use. J Biomater Appl. 1999; 14(2):184–191. [PubMed: 10549004]
65. Patel A, Gaharwar AK, Iviglia G, Zhang H, Mukundan S, Mihaila SM, Demarchi D, Khademhosseini A. Highly elastomeric poly(glycerol sebacate)-co-poly(ethylene glycol) amphiphilic block copolymers. Biomaterials. 34(16):3970–3983. [PubMed: 23453201]

66. Yan LP, Oliveira JM, Oliveira AL, Caridade SG, Mano JF, Reis RL. Macro/microporous silk fibroin scaffolds with potential for articular cartilage and meniscus tissue engineering applications. Acta Biomater. 8(1):289–301. [PubMed: 22019518]

67. Park JS, Woo DG, Sun BK, Chung HM, Im SJ, Choi YM, Park K, Huh KM, Park KH. In vitro and in vivo test of PEG/PCL-based hydrogel scaffold for cell delivery application. Journal of controlled release : official journal of the Controlled Release Society. 2007; 124(1–2):51–59. [PubMed: 17904679]

68. Ju YM, Park K, Son JS, Kim JJ, Rhie JW, Han DK. Beneficial effect of hydrophilized porous polymer scaffolds in tissue-engineered cartilage formation. J Biomed Mater Res B Appl Biomater. 2008; 85(1):252–260. [PubMed: 17973245]

69. Park H, Guo X, Temenoff JS, Tabata Y, Caplan AI, Kasper FK, Mikos AG. Effect of swelling ratio of injectable hydrogel composites on chondrogenic differentiation of encapsulated rabbit marrow mesenchymal stem cells in vitro. Biomacromolecules. 2009; 10(3):541–546. [PubMed: 19173557]

70. Karageorgiou V, Tomkins M, Fajardo R, Meinel L, Snyder B, Wade K, Chen J, Vunjak-Novakovic G, Kaplan DL. Porous silk fibroin 3-D scaffolds for delivery of bone morphogenetic protein-2 in vitro and in vivo. J Biomed Mater Res A. 2006; 78(2):324–334. [PubMed: 16637042]

71. Kleinheinz J, Jung S, Wermker K, Fischer C, Joos U. Release kinetics of VEGF165 from a collagen matrix and structural matrix changes in a circulation model. Head & face medicine. 2010; 6:17. [PubMed: 20642842]

72. Uebersax L, Merkle HP, Meinel L. Insulin-like growth factor I releasing silk fibroin scaffolds induce chondrogenic differentiation of human mesenchymal stem cells. Journal of controlled release : official journal of the Controlled Release Society. 2008; 127(1):12–21. [PubMed: 18280603]

73. Niu X, Feng Q, Wang M, Guo X, Zheng Q. Porous nano-HA/collagen/PLLA scaffold containing chitosan microspheres for controlled delivery of synthetic peptide derived from BMP-2. Journal of controlled release : official journal of the Controlled Release Society. 2009; 134(2):111–117. [PubMed: 19100794]

74. Kanczler JM, Barry J, Ginty P, Howdle SM, Shakesheff KM, Oreffo RO. Supercritical carbon dioxide generated vascular endothelial growth factor encapsulated poly(DL-lactic acid) scaffolds induce angiogenesis in vitro. Biochemical and biophysical research communications. 2007; 352(1):135–141. [PubMed: 17112464]

75. Guerne PA, Carson DA, Lotz M. IL-6 production by human articular chondrocytes. Modulation of its synthesis by cytokines, growth factors, and hormones in vitro. J Immunol. 1990; 144(2):499–505. [PubMed: 2104896]

76. Ryu JH, Yang S, Shin Y, Rhee J, Chun CH, Chun JS. Interleukin-6 plays an essential role in hypoxia-inducible factor 2alpha-induced experimental osteoarthritic cartilage destruction in mice. Arthritis Rheum. 63(9):2732–2743. [PubMed: 21590680]

77. Ousema PH, Moutos FT, Estes BT, Caplan AI, Lennon DP, Guilak F, Weinberg JB. The inhibition by interleukin 1 of MSC chondrogenesis and the development of biomechanical properties in biomimetic 3D woven PCL scaffolds. Biomaterials. 33(35):8967–8974. [PubMed: 22999467]

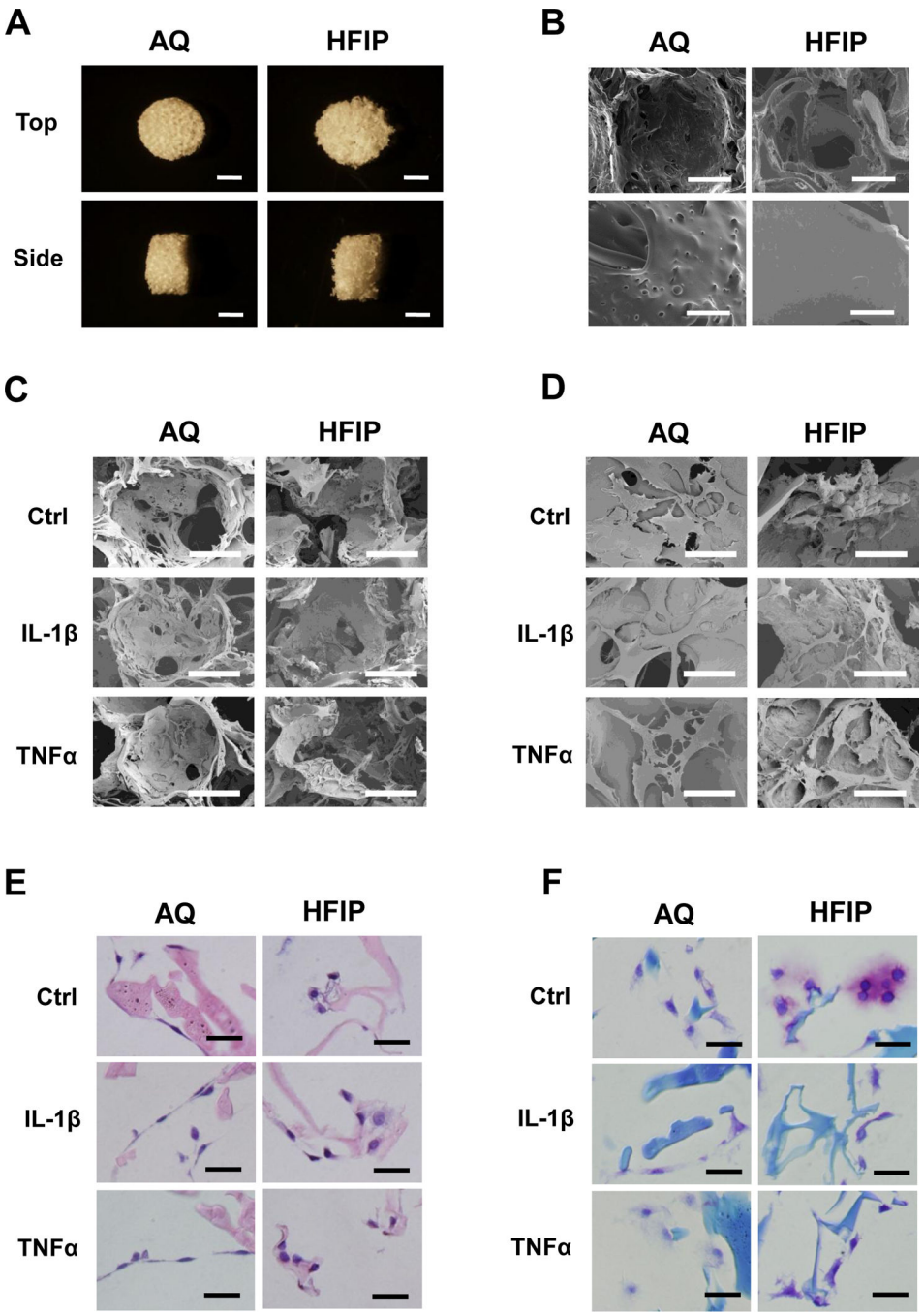

Fig. 1. Morphological and histological characterization of chondrocytes in AQ and HFIP silk scaffolds

(A) Bright field images of AQ and HFIP silk scaffolds. Top views (top panels) and side views (bottom panels) of the scaffolds. Scale bars: 2mm. **(B)** Scanning electron microscopic (SEM) images of AQ and HFIP silk scaffolds. Top panels: low magnification, scale bar: 200μm. Bottom panel, high magnification, scale bar: 40μm. **(C)** Low magnification SEM images of bovine articular chondrocytes inside the scaffolds after 16 days of culture, scale bar: 200μm. **(D)** High magnification SEM images of chondrocytes inside the scaffolds after

16 days of culture. Scale bar: 50μm. **(E)** H&E staining of chondrocytes in AQ and HFIP silk scaffolds. Scale bar: 25μm. **(F)** Toluidine Blue staining in chondrocytes in AQ and HFIP scaffolds. Scale bar: 25μm. For **C–F**: Ctrl (no cytokine added), IL-1β (10ng/ml), and TNFα (10ng/ml).

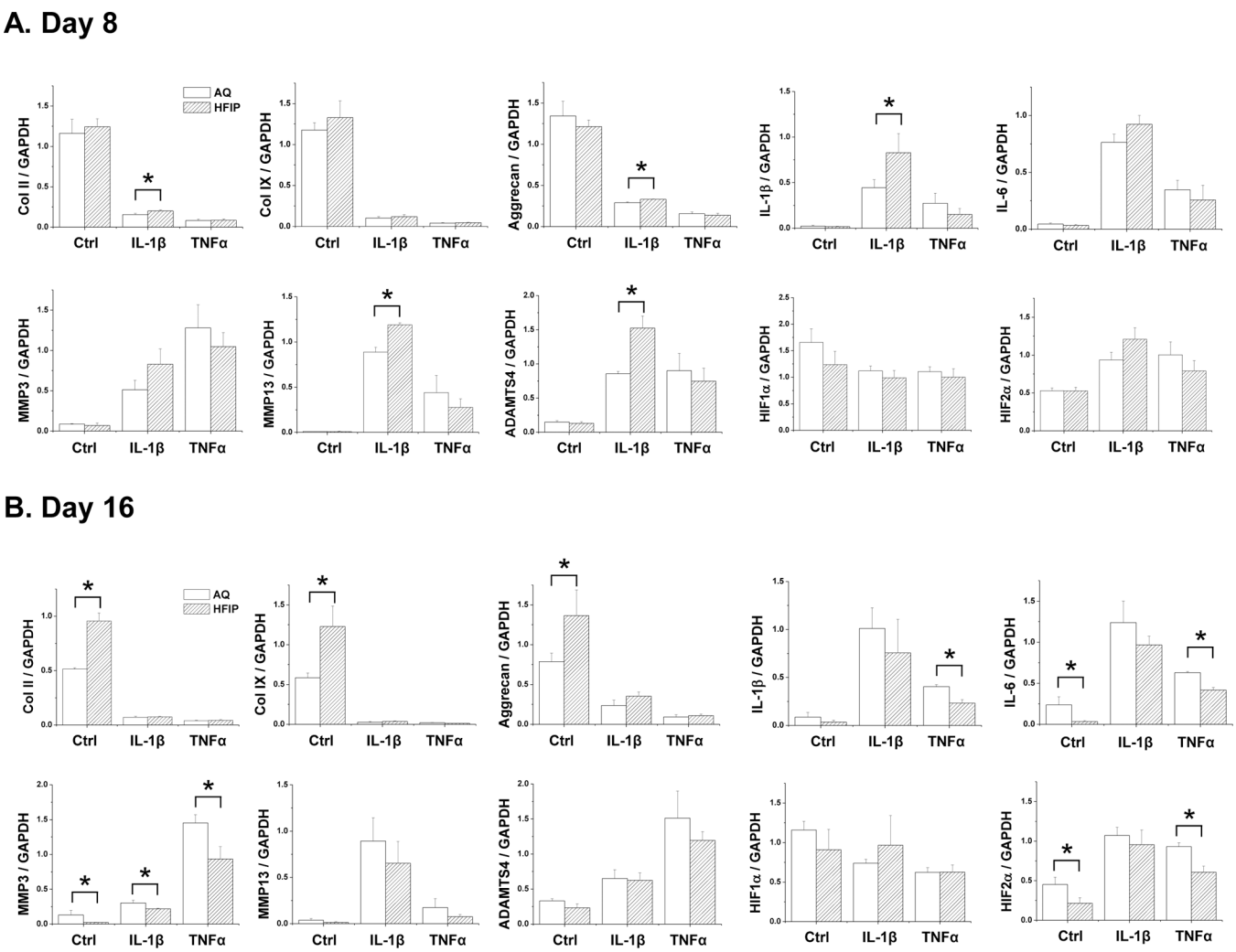

Fig. 2. qRT-PCR Gene expression analysis of chondrocytes grown in AQ and HFIP silk scaffolds

Bovine articular chondrocytes were grown in AQ and HFIP silk scaffolds for 8 or 16 days with the following treatment: control (no cytokine treatment), IL-1β (10ng/ml) and TNFα (10ng/ml). The expression of the following genes was analyzed: collagen II (Col II), collagen IX (Col IX), aggrecan, endogenous IL-1β, IL-6, MMP3, MMP13, ADAMTS4, HIF1α and HIF2α. For each treatment, results from three independent samples are shown. **(A)** Results from Day 8 cultures. **(B)** Results from Day 16 cultures. All gene expression levels were normalized to GAPDH. Data present mean ± SD. *p<0.05.

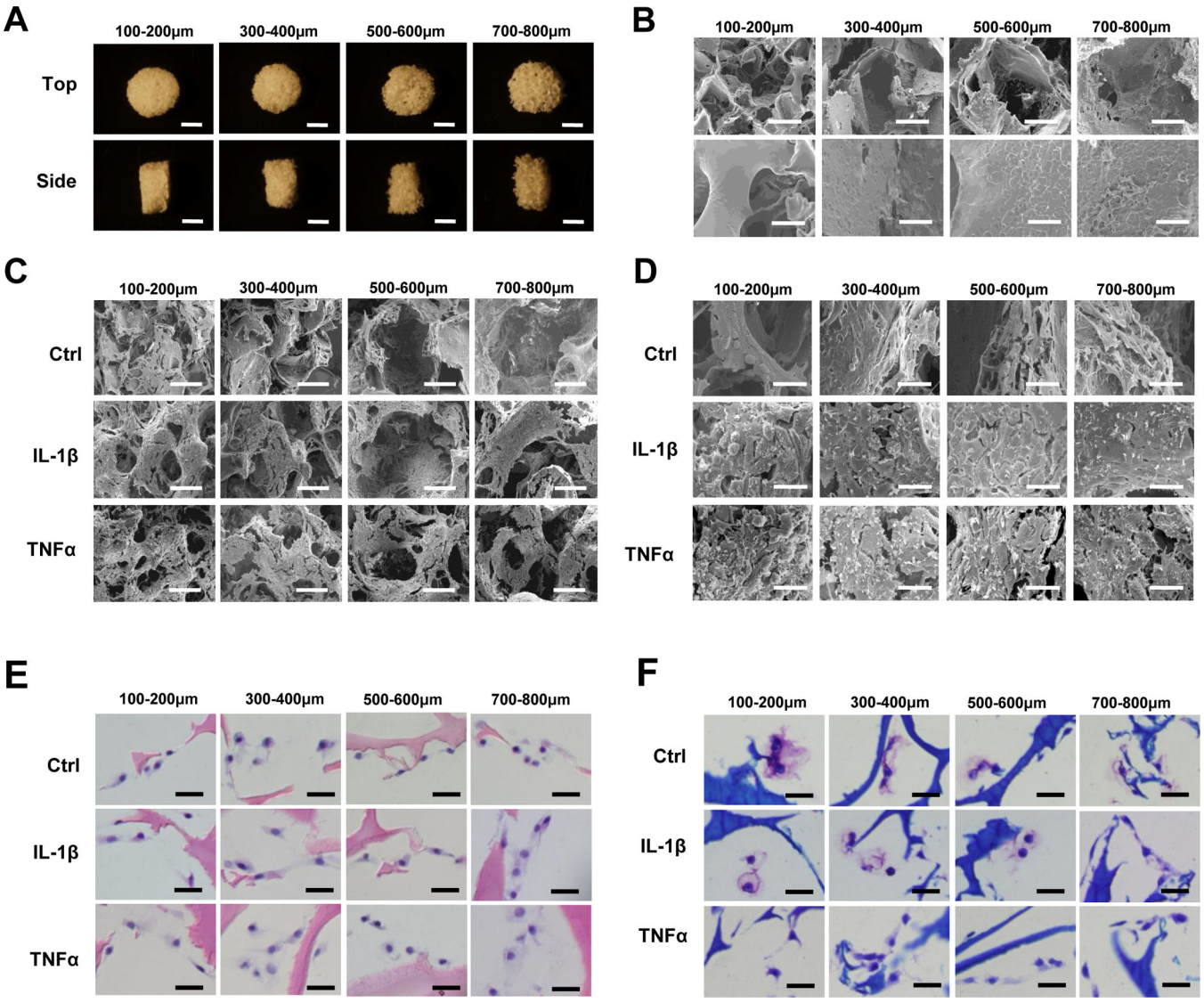

Fig. 3. Morphological and histological characterization of chondrocytes in HFIP silk scaffolds of different pore sizes

(A) Bright field images of HFIP silk scaffolds with pore sizes of 100–200μm, 300–400μm, 500–600μm, and 700–800μm. Top views (top panels) and side views (bottom panels) of the scaffolds. Scale bars: 2mm. **(B)** SEM micrographs of HFIP silk scaffolds with these pore sizes. Top panels: low magnification, scale bar: 200μm. Bottom panel, high magnification, scale bar: 40μm. **(C)** Low magnification SEM images of chondrocytes inside the scaffolds after 16 days of culture, scale bar: 200μm. **(D)** High magnification SEM images of chondrocytes inside the scaffolds after 16 days of culture, scale bar: 40μm. **(E)** H&E staining of chondrocytes in HFIP silk scaffolds of different pore sizes after 16 days of culture. Scale bar: 25μm. **(F)** Toluidine Blue staining of chondrocyte seeded in HFIP silk scaffolds of different pore sizes after 16 days of culture. Scale bar: 25μm. For **C–F**: Ctrl (no cytokine added), IL-1β (10ng/ml), and TNFα (10ng/ml).

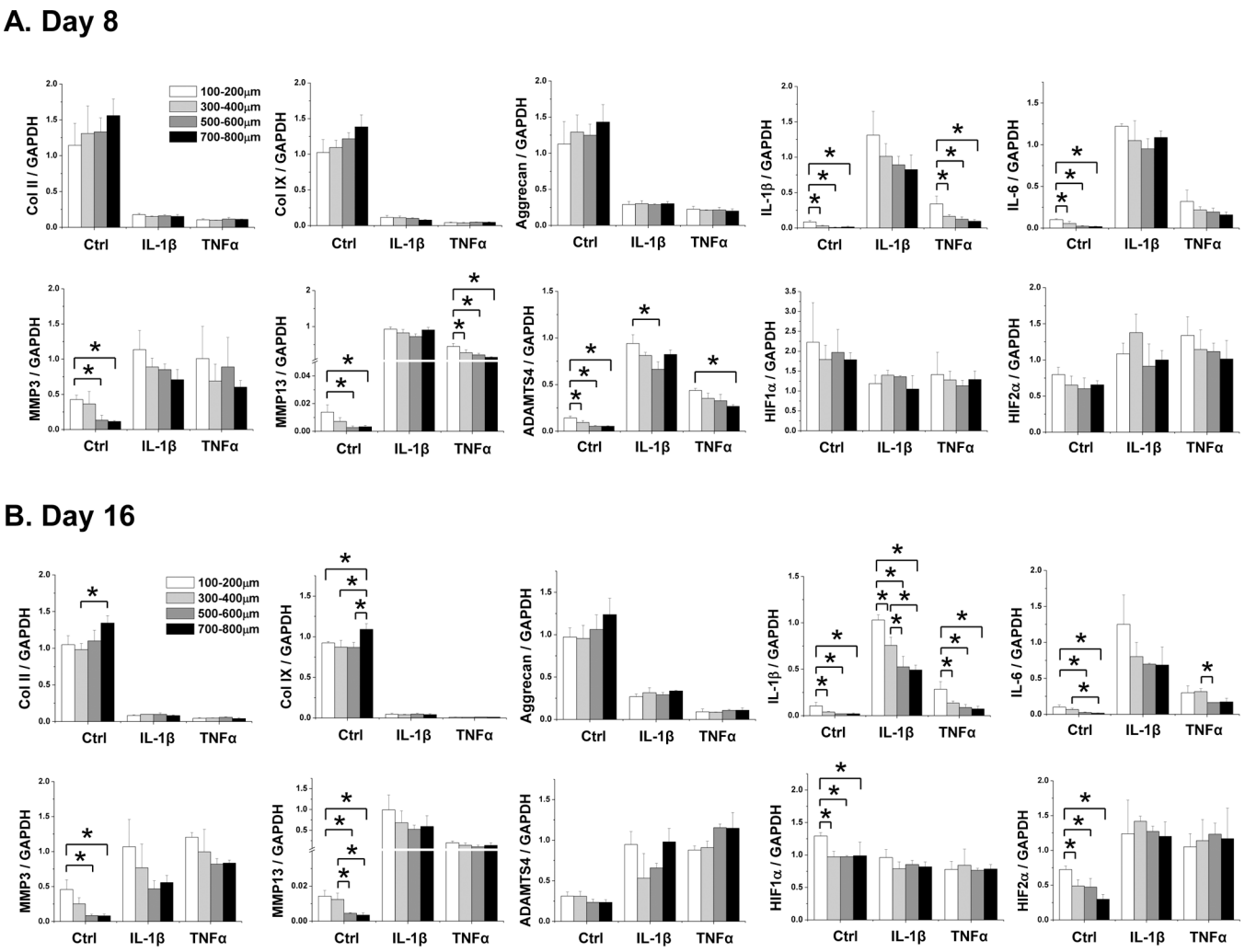

Fig. 4. qRT-PCR Gene expression analysis of chondrocytes grown in HFIP silk scaffolds of different pore sizes

Bovine articular chondrocytes were grown in AQ and HFIP silk scaffolds for 8 or 16 days with the following treatment: control (no cytokine treatment), IL-1β (10ng/ml) and TNFα (10ng/ml). The expression of the following genes was analyzed: collagen II (Col II), collagen IX (Col IX), aggrecan, endogenous IL-1β, IL-6, MMP3, MMP13, ADAMTS4, HIF1α and HIF2α. For each treatment, results from three independent samples are shown. **(A)** Results from Day 8 cultures. **(B)** Results from Day 16 cultures. All gene expression levels were normalized to GAPDH. Data present mean ± SD. *p<0.05.

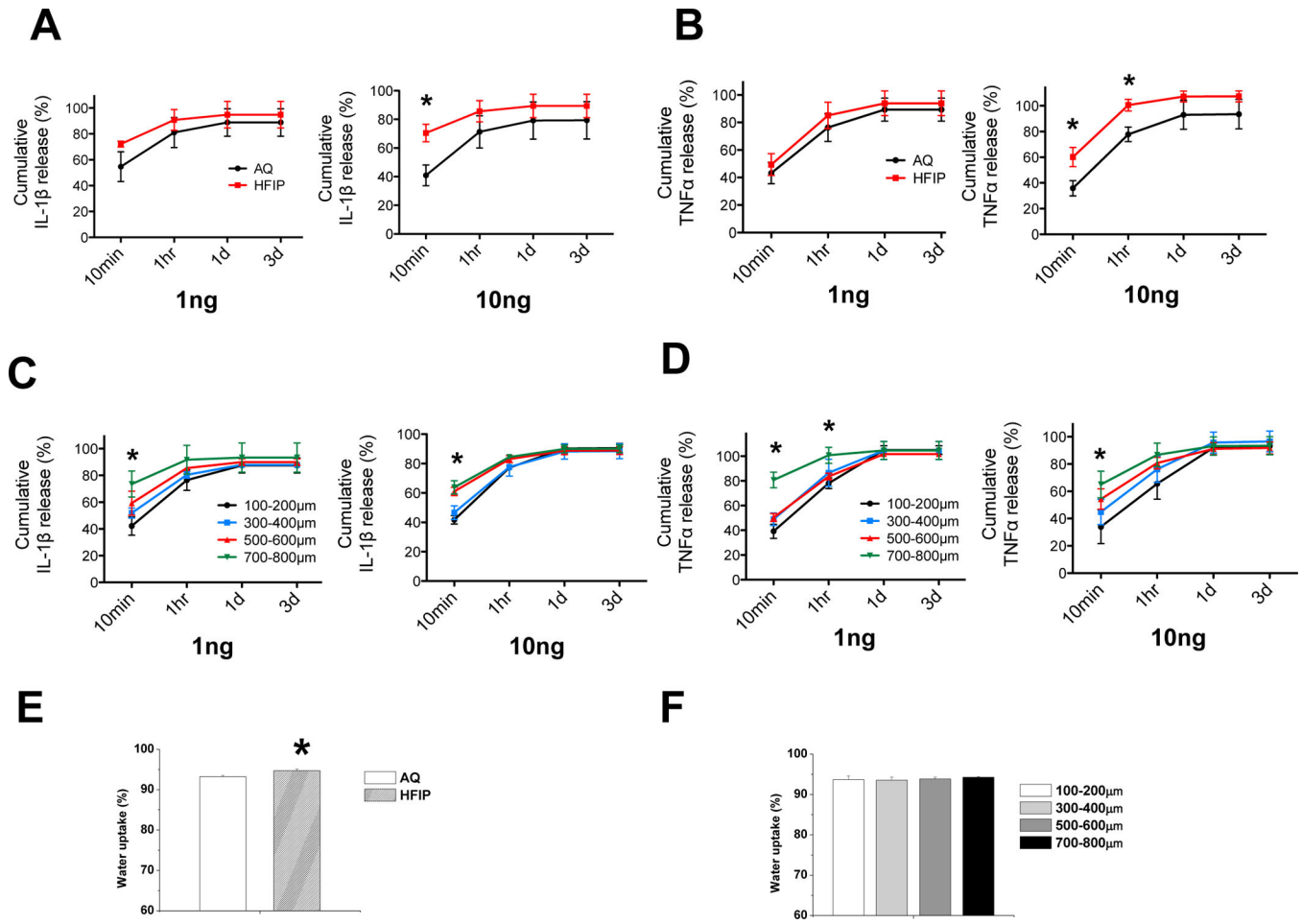

Fig. 5. Evaluation of kinetics of scaffolds in releasing pro-inflammatory cytokines and water uptake properties of the scaffolds

(A–D) Two different amounts of pro-inflammatory cytokines IL-1β or TNFα (1 and 10ng) were loaded onto empty prewetted AQ and HFIP scaffolds, as well as HFIP with different pore sizes, and scaffolds were placed into the culture medium. At 4 different time points: 10min, 1hr, 1 day, and 3 days, the amount of IL-1β or TNFα leached from the scaffolds into the medium were evaluated by ELISA. Percent release was calculated as the ratio of the amount of cytokines in the medium to the total amount of cytokines loaded onto the scaffolds. Percent cumulative release was calculated as the ratio of cumulative amount of cytokines in the medium at each time point (i.e. sum of mass of cytokines at each time point and all prior time points) to the total amount of cytokines loaded onto the scaffolds. **(A)** Percent release and cumulative release analyses of IL-1β from AQ and HFIP silk scaffolds at each time point. **(B)** Percent release and cumulative release analyses of TNFα from AQ and HFIP silk scaffolds at each time point. **(C)** Percent release and cumulative release analyses of IL-1β from HFIP silk scaffolds with different pore sizes at each time point. **(D)** Percent release and cumulative release analyses of TNFα from HFIP silk scaffolds with different pore sizes at each time point. **(E–F)** Water uptake properties of AQ, HFIP, and HFIP silk scaffolds with different pore sizes were examined. **(E)** Water uptake (%) analyses of AQ and

HFIP silk scaffolds. **(F)** Water uptake (%) analyses of HFIP silk scaffolds with different pore sizes. Data present mean ± SD. *p<0.05.